SLAC-PUB-13224
arXiv:0804.4608v1[hep-ph]
April 2008

The Baryon Anomaly: Evidence for Color Transparency and Direct Hadron Production at RHIC

Stanley J. Brodsky

Stanford Linear Accelerator Center, Stanford University, Stanford, California 94309

Anne Sickles

Brookhaven National Laboratory, Upton, New York 11973

Abstract

We show that the QCD color transparency of higher-twist contributions to inclusive hadroproduction cross sections, where baryons are produced directly in a short-distance subprocess, can explain several remarkable features of high-p_T baryon production in heavy ion collisions which have recently been observed at RHIC: (a) the anomalous increase of the proton-to-pion ratio with centrality (b): the increased power-law fall-off at fixed $x_T = 2p_T/\sqrt{s}$ of the charged particle production cross section in high centrality nuclear collisions, and (c): the anomalous decrease of the number of same-side hadrons produced in association with a proton trigger as the centrality increases. We show that correlations between opposite-side hyperons and kaons can provide a clear signature of higher-twist contributions. These phenomena emphasize the importance of understanding hadronization at the amplitude level in QCD illustrate how heavy ion collisions can provide sensitive tools for interpreting and testing fundamental properties of QCD.

1 Introduction

One of the most surprising results observed at RHIC is the behavior of the ratio of protons to pions produced at large transverse momenta in heavy ion collisions. Intuitively, one would expect that protons and other baryons would be depleted relative to mesons as the overlap of the colliding nuclei is increased. However, as shown in Fig. 1, the p/π and $\bar{p}/\pi$ ratio at $p_T \sim 4$ GeV/c measured at RHIC increases with the centrality of the heavy ion collision.

Work supported in part by US Department of Energy contract DE-AC02-76SF00515

The standard perturbative QCD approach to hadron production at large transverse momentum is based on elementary leading-twist $2 \to 2$ quark and gluon hard scattering processes followed by jet hadronization. For p_T >2 GeV/c the π^0 [1] spectra in p+p collisions at $\sqrt{s}$=200 GeV appear to be well described by next to leading order pQCD calculations. In Au+Au collisions the produced high transverse momentum quarks and gluons must also traverse a zone of hot nuclear medium [2,3,4,5]. The scattered partons then lose energy traversing the dense colored matter and fragment into hadrons far from the collision region according to the same fragmentation process as in p+p collisions. In this scenario the ratio of particles as a function of p_T should be nearly independent of the collision system. However, the data [6,7] show large modifications of the particle ratios for 2< p_T <6 GeV/c.

Additional information on the anomalous baryon-to-meson particle ratios can be obtained by studying the correlations between the produced hadron and other hadrons produced on the same side at nearby rapidities [8,9]. These correlations show an unexpected dependence on particle type. The number of particles associated with a meson ($\pi^{\pm}$,$K^{\pm}$) at $2.5 < p_T < 4.0$ GeV/c increases linearly with the number of nucleons from the incoming nuclei participating in the collision, N_{part}. This increase is qualitatively understood as the lost energy from the parton producing additional hadrons correlated with the jet direction. In contrast the number of particles associated with a high p_T proton or anti-proton trigger decreases with N_{part} in the most central collisions; see Fig. 2. This anomalous difference between the nuclear dependence of pion and proton production are inconsistent with the standard perturbative QCD picture of hard scattering followed by vacuum fragmentation.

The increased baryon/meson ratios in Au+Au collisions have been explained by attributing final state hadron formation for 2< p_T <6 GeV/c to quark coalescence [10,11,12]. In these models quarks (and anti-quarks) close in phase space recombine to form the final state hadrons. Such models favor baryons, with three valence quarks, since the hadron momentum is the sum of the quark momenta. However, these models have not been able to explain the centrality and particle type dependence of same side correlations [13,14].

We propose that the large baryon/meson ratios at RHIC collisions are the result of baryons directly produced in the hard scattering through higher-twist subprocesses such as $qq \to B\bar{q}$. The baryon is initially produced in a color-singlet configuration; its transverse size is small reflecting the high transverse momenta exchanged within the subprocess. Higher-twist baryon and anti-baryon production should occur in both p+p and Au+Au collisions. However, in Au+Au collisions the small size of the baryons should enable them to traverse the matter with minimal interactions as predicted by color transparency. The medium in Au+Au collisions then acts as a filter; partons from leading-twist scattering are suppressed by losing energy and those produced

in direct processes remain.

Higher-twist semi-exclusive subprocesses [15] where hadrons interact directly in the hard subprocess are a natural feature of QCD. Multi-parton and semi-exclusive subprocesses underly the analysis of hard exclusive processes such as deeply virtual Compton scattering, deeply virtual meson production, fixed-angle scattering, and elastic and inelastic form factors at large momentum transfer. A particularly important example for inclusive reactions is the Drell-Yan process $\pi p \to \gamma^* X$ where the direct $n_{active=5}$ higher-twist subprocess $\pi q \to \gamma^* q$ dominates lepton pair production at high x_F, explaining the constant behavior of the cross section as a function of the parton momentum fraction and the observed dominance of longitudinally polarized virtual photons [16]. The higher-twist amplitude is decreased by a factor of f_π/Q relative to the leading-twist amplitude; however this is over-compensated by the lack of phase space suppression of the direct process at $x_F \to 1$. The non-perturbative wavefunction which controls the direct higher-twist process $\pi q \to \gamma^* q$ is the gauge invariant and frame-independent pion distribution amplitude [17] $\phi_\pi(x)$. The shape and normalization of hadronic distribution amplitudes can now be predicted using the AdS/QCD correspondence [18].

2 Scaling Behavior of Hard Hadron Production in QCD

The most important discriminant of the twist of a pQCD subprocess in a hard hadronic collision is the scaling of the inclusive cross section

$$\frac{d\sigma}{d^3p/E}(pp \to HX) = \frac{F(x_T, \theta_{cm})}{p_T^n}$$

at fixed $x_T = 2p_T/\sqrt{s}$ and θ_{cm} In the original parton model [19] the power fall-off is simply $n = 4$ since the underlying $qq \to qq$ subprocess amplitude for point-like partons is scale invariant, and there is no dimensionful parameter in the theory. The Bjorken scaling of the deep inelastic lepton cross section $\ell p \to \ell' X$ is based on the same scale-invariance principle. In a full perturbative QCD analysis based on 2-to-2 quark and gluon subprocesses, the scale-invariance of the inclusive cross section is broken by the logarithmic running of the running coupling and the evolution of the structure functions and fragmentation functions. These effects increase the prediction for n to $n = 4.5 \to 5$ as illustrated in Fig. 3 [20].

There have been extensive measurements of inclusive hadron production cross sections, particularly from the CERN ISR and fixed-target experiments at Fermilab. As summarized by Cronin in his 1974 review [21], the cross sections measured for $pp \to \pi X$ and $pp \to pX$ are far from scale-invariant. See Fig.

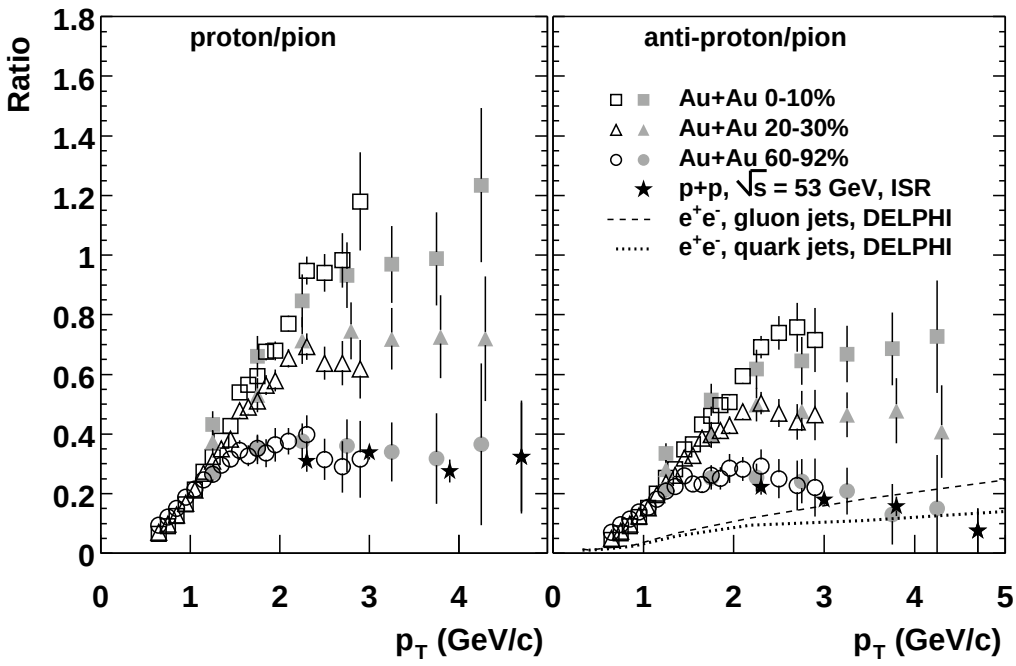

Fig. 1. Ratio of proton to pion and anti-proton to pion production as a function of p_T for Au-Au collisions at at $\sqrt{s} = 200$ GeV for different centrality. The p/π and $\bar{p}/\pi$ ratio increase as collisions between the incoming nuclei become more central (the impact parameter decreases). Open and filled symbols represent charged and neutral pions, respectively. The stars show the particle ratio for pp collisions at $\sqrt{s} = 53$ GeV. The ratio for quark and gluon jet fragmentation are also shown. From Ref. [6]

4. The power fall-off at fixed x_T is consistent with the leading-twist pQCD prediction $n = 4.5 \to 5$ only at the very smallest values of x_T. In fact, n is not a constant power ; it is observed to be a monotonically increasing function of x_T, reaching $n = 20$ for $pp \to pX$ at the exclusive limit $x_T \to 1$.

In the case of RHIC, the shape of the inclusive cross section for pion production measured in peripheral collisions at $\sqrt{s} = 200$ GeV [22] appears to be in general agreement with NLO leading-twist QCD expectations [1]. However, as seen in Fig. 5, the scaling of the pion data at fixed x_T for $0.03 < x_T < 0.06$ shows a rising behavior of $n(x_T)$ with an average value $n \sim 6.4 \pm 0.5$ [22]. Fig. 1 also shows that the proton-to-pion and anti-proton to meson ratios measured in peripheral and central heavy ion collisions differ from that of quark and gluon jets in e^+e^- annihilation [6]. This breakdown of factorization also suggests that a description of the heavy ion hadroproduction data based solely on leading-twist contributions is not adequate. In contrast, the photon production cross section [23,24] $pp \to \gamma X$ at fixed x_T scales over a large range of energies with a constant power $n \sim 5$ at $x_T < 0.04$, consistent with the

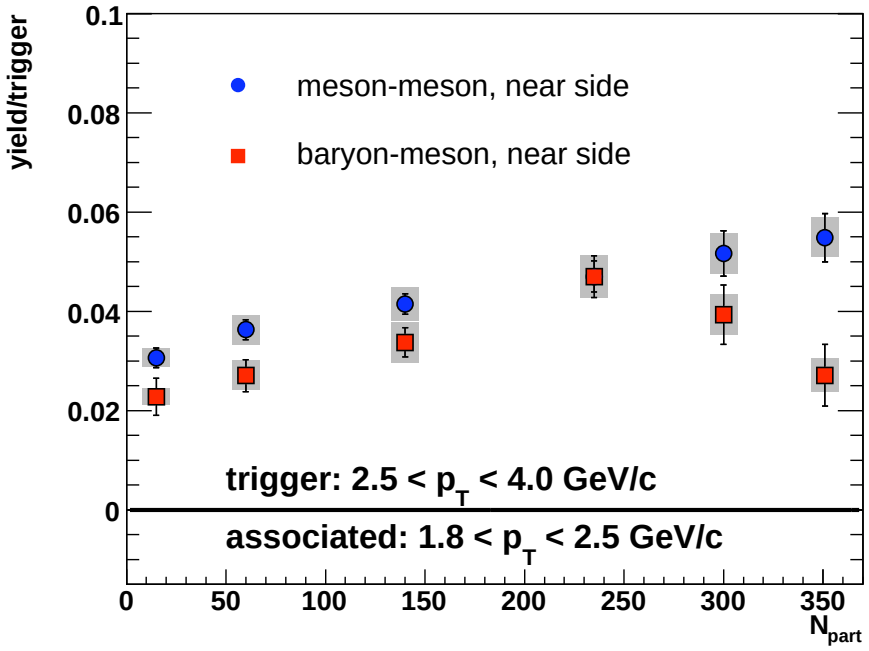

Fig. 2. Same-side and away side correlated hadrons for meson and baryon triggers as a function of N_{part}. The number of same-side particles associated with a meson trigger increases monotonically with the size of the collision system. In contrast, he number of same-side particles associated with a proton trigger decreases as N_{part} increases. From Ref. [9]

leading-twist pQCD prediction based on the $gq \to q\gamma$ subprocess. The direct comparison of the γ/π ratio with theory at fixed x_T would be illuminating; if the leading-twist description is correct, the ratio should be nearly scale-invariant except for small corrections from jet fragmentation and the running coupling. The choice of renormalization scale for each subprocess, including the non-Abelian couplings, can be fixed using the BLM method [25,26], thus eliminating one source of ambiguity of the leading-twist predictions.

The seemingly anomalous scale-breaking behavior for hadroproduction can be naturally explained if in addition to the leading-twist processes, there are also contributions from "higher-twist" (multi-parton) processes. As x_T increases, it becomes more advantageous to produce the trigger hadron directly in a semi-exclusive hard subprocess [15] such as $gq \to \pi q$ or $qq \to p\bar{q}$, since this avoids any waste of energy from jet fragmentation [27]. An example is illustrated in Fig. 6. It is also more energy efficient to scatter more than one parton in the projectile, such as $q + (qq) \to q(qq)$ followed by fragmentation of the diquark to the trigger proton. In each case the penalty of the extra fall-off in p_T from hadron compositeness or the diquark correlation scale is compensated by a lesser fall-off in x_T.

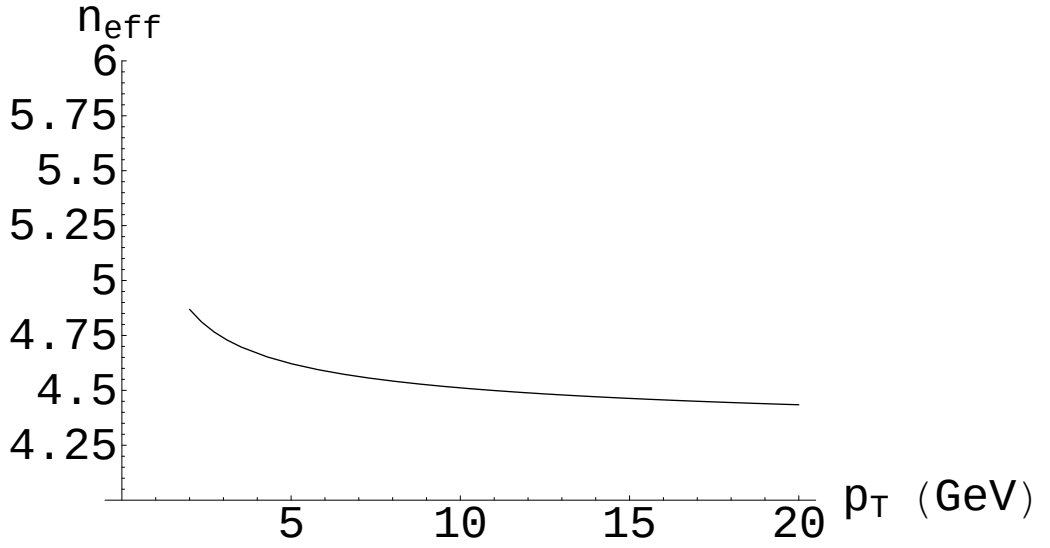

Fig. 3. Modification of scale-invariance from the logarithmic running of the QCD coupling constant and DGLAP evolution. From Ref. [20]

Dimensional counting rules provide a simple rule-of-thumb guide for the power-law fall-off of the inclusive cross section in both p_T and $(1-x_T)$ due to a given subprocess [28]:

$$E\frac{d\sigma}{d^3p}(AB \to CX) \propto \frac{(1-x_T)^{2n_{spectator}-1}}{{p_T}^{2n_{active}-4}}$$

where n_{active} is the "twist", i.e., the number of elementary fields participating in the hard subprocess, and $n_{spectator}$ is the total number of constituents in A, B and C not participating in the hard-scattering subprocess. For example, consider $pp \to pX$. The leading-twist contribution from $qq \to qq$ has $n_{active} = 4$ and $n_{spectator} = 6$. The higher-twist subprocess $qq \to p\bar{q}$ has $n_{active} = 6$ and $n_{spectator} = 4$. This simplified model provides two distinct contributions to the inclusive cross section

$$\frac{d\sigma}{d^3p/E}(pp \to pX) = A\frac{(1-x_T)^{11}}{p_T^4} + B\frac{(1-x_T)^7}{p_T^8} \tag{1}$$

and $n = n(x_T)$ increases from 4 to 8 at large x_T.

In a general QCD analysis of inclusive hadroproduction one needs to sum over all contributing leading and higher-twist hard subprocesses. At $x_T = 1$ the quarks in the protons must all scatter in an $n_{active} = 12, n = 20, n_{spectator} = 0$ exclusive subprocess. In each case the nominal fall-off given by counting rules will be increased by the running of the QCD coupling and either DGLAP evo-

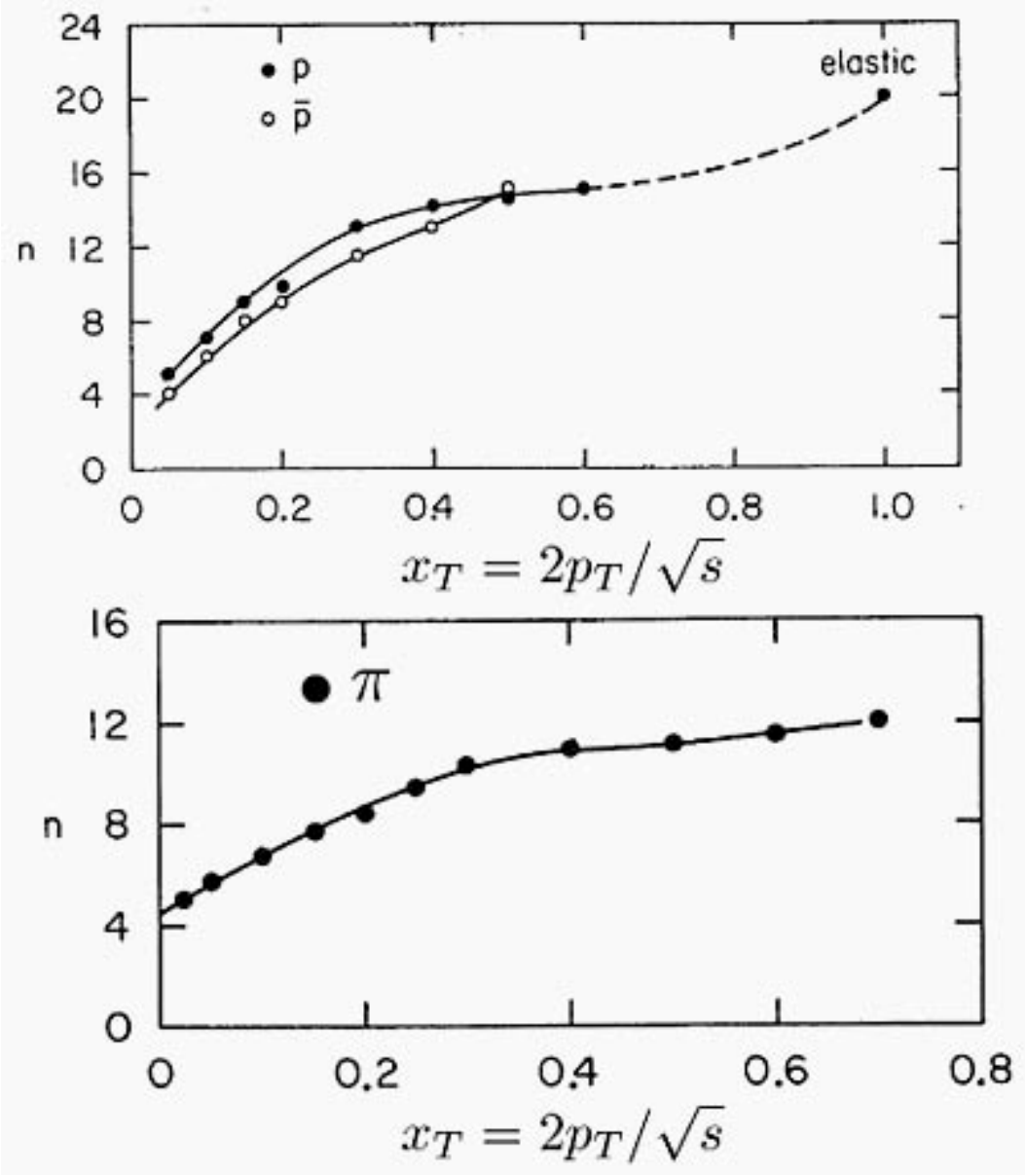

Fig. 4. Effective power-law fall-off of the inclusive cross section for proton, anti-proton and pion hadroproduction at fixed x_T and fixed θ_{cm}. From Ref. [21].

lution of the structure functions or ERBL evolution [17,29] of the distribution amplitudes for the directly-interacting hadrons. Although large p_T hadron production at RHIC is most likely dominated by leading-twist QCD processes [30], higher-twist subprocesses can play a significant role, particularly in the case of proton production.

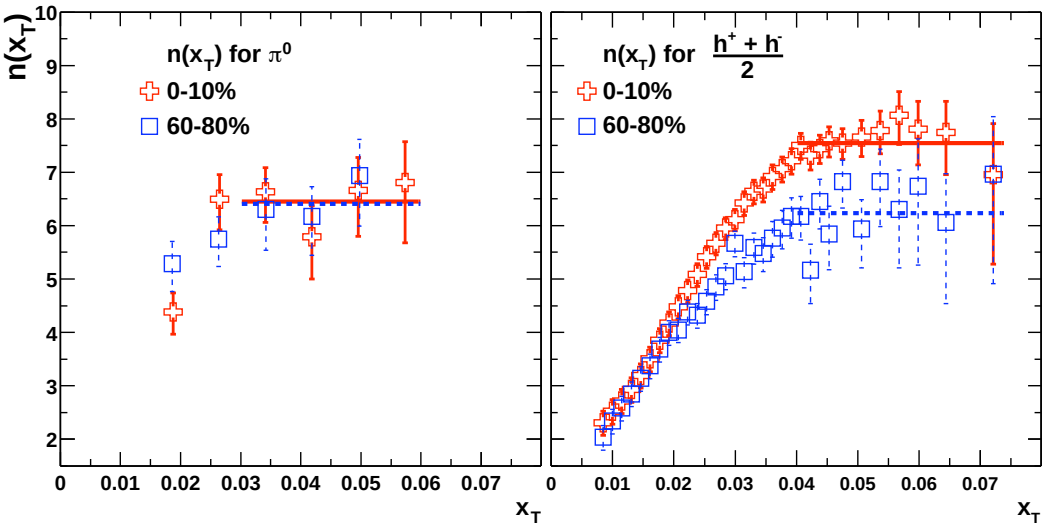

Fig. 5. Effective power-law fall-off of the inclusive cross section for π^0 and charged particle hadroproduction at fixed x_T and fixed θ_{cm} at RHIC energies. The power law increases as a function of x_T and is different for central and peripheral collisions in the case of charged particle production. The charged hadrons include protons and anti-protons. From Ref. [22]

3 Color Transparency

In higher-twist subprocesses such as $gq \to \pi q$, $\pi q \to \gamma^* q$ or $qq \to p\bar{q}$, the wavefunction of a hadron enters directly into the amplitude. The dominant contribution comes from fluctuations of the hadronic wavefunction where the quarks in the valence Fock state are at small impact separation $b_\perp \sim 1/p_T$. Interactions with the external system are thus suppressed unless the wavelength of the exchanged gluon is comparable to the transverse size of the color singlet system; i.e. $k_\perp \sim p_\perp$ The small-size color-singlet configurations of the hadron can thus propagate through the nuclear medium with minimal hadronic interactions; i.e. they are *color transparent* [31].

Color transparency [32,33] is a fundamental property of QCD as a gauge theory of hadronic interactions. A clear empirical demonstration has been given in diffractive di-jet production $\pi A \to \text{jetjet}A'$ by the E791 experiment at Fermilab [34]; the forward amplitude for the diffractive production of high transverse momentum di-jets is found to scale as A^α where $\alpha \simeq 1$; i.e. the diffractive di-jet production amplitude is coherent on every nucleon in the nucleus. This is in dramatic contradiction to traditional Glauber theory where only nucleons on the periphery of the nucleus are effective. Color transparency predictions for quasi-elastic pion electoproduction $eA \to e'\pi^+ X$ have recently been verified at Jefferson Laboratory [35].

Color transparency provides an appealing explanation of the anomalous baryon

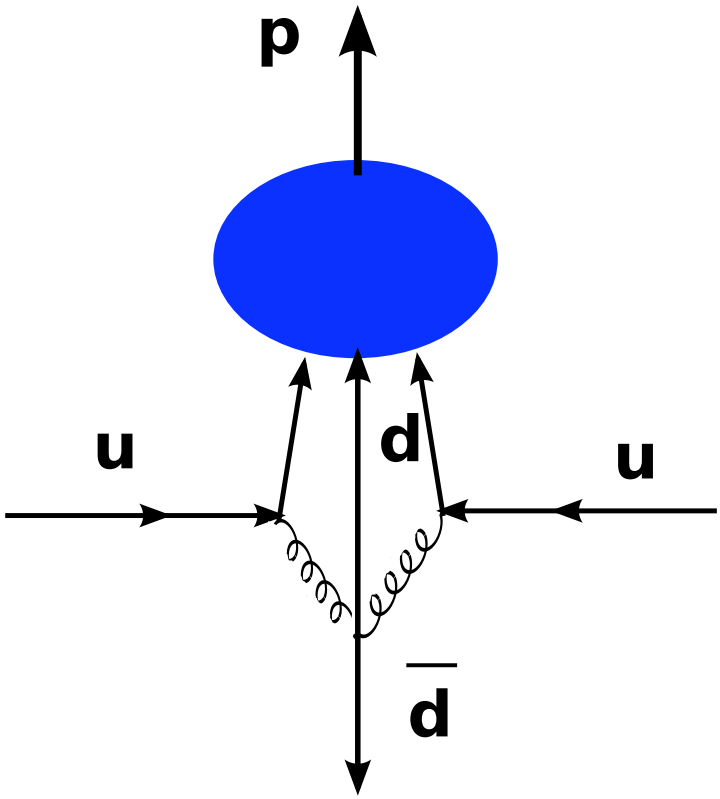

Fig. 6. Higher-twist contribution to proton production at high p_T. The proton is produced directly within the 6-parton hard subprocess.

to meson ratios observed at RHIC. For simplicity, let us assume the two-component model for $pp \to pX$ given in Equation 1. The higher-twist term due to $qq \to p\bar{q}$ produces an isolated proton as a small color singlet which is unaffected by the nuclear environment; in contrast, the leading-twist term produces a high p_T parton which propagates through the matter and loses energy. The fragmentation process further suppresses the leading-twist term because the p_T carried by the parton is spread between many hadrons. The increased relative contribution of higher-twist baryon production leads to the higher effective power n for charged hadrons seen in Fig. 5.

Furthermore, since the increased importance of higher-twist contributions to the proton and anti-proton production cross section in highly central events ($N_{part} > 250$), we can also understand why the number of same side hadrons correlated with a the baryon trigger decreases (Fig. 2). The directly produced proton interacts much less in the nuclear medium than a proton produced via jet fragmentation. In contrast, the meson trigger does not show this effect; the

number of same-side mesons increase monotonically with N_{part}.

Direct p and $\bar{p}$ production could also explain higher p_T (p_T >6 GeV/c) measurements at RHIC [36]. Expectations from pQCD are that gluons passing through colored matter will lose more energy than quarks because of the larger color factor; energy loss for a gluon should be 9/4 larger than for a quark. At RHIC over 90% of p and $\bar{p}$ produced via leading-twist scattering at 6< p_T <12 GeV/c are expected to come from gluon fragmentation. In contrast, approximately half of the pions are expected from gluon fragmentation[37,38]. Because of the dominance of gluon jets, p and $\bar{p}$ spectra should be more suppressed than the pion spectra[39]. The data, however, show that even for 6< p_T <12 GeV/c pions are more suppressed in central Au+Au collisions. While the cross section for higher-twist processes falls off with a higher power in p_T than leading-twist processes, there could still be significant contributions from direct p and $\bar{p}$ production. As seen in Equation 1, while the fall off of the higher-twist term is, in part, balanced by the lesser fall off in x_T.

The $pp \rightarrow \pi X$ cross section also receives leading-twist fragmentation and direct higher-twist contributions from $gq \rightarrow \pi q$, etc.; however, as seen from the power fall-off of $n(x_T)$ shown in Fig. 4, higher-twist processes are evidently relatively more significant for proton compared to pion triggers in the RHIC kinematic domain. Thus color transparency and direct hadron production is mostly associated with proton and other baryon triggers.

4 Predictions for Baryons Containing s and $\bar{s}$ Quarks

Higher-twist processes are also expected to contribute to hyperon production. For example, a Λ can be produced directly at large transverse momentum via the semi-exclusive subprocess $ud \rightarrow \Lambda\ \bar{s}$ in analogy to the $uu \rightarrow p\bar{d}$ subprocess illustrated in Fig. 6. In the case of Λ production, the s and $\bar{s}$ are in opposing di-jets. In contrast, in leading-twist parton scattering the strangeness of particles in the opposing di-jets should be independent. Measurements of correlations between hyperons and charged kaons would be a clear signature of baryon production via higher-twist subprocesses. In that case, there should be an excess of Λ-K^+ and $\bar{\Lambda}$-K^- correlations over Λ-K^- and $\bar{\Lambda}$-K^+ correlations when the hyperon and kaon are in opposing di-jets. The strength of this correlation should change with the relative contribution from direct and fragmentation processes for Λ production; measurements of the centrality and p_T^{Λ} dependence will constrain the contribution of direct processes to baryon production. These correlations would not be naturally explained by quark coalescence models and would provide a means of distinguishing between different baryon production mechanisms.

5 Conclusions

We have shown that the QCD color transparency of higher-twist contributions to inclusive hadroproduction cross sections, where baryons are produced directly in a short-distance subprocess, can explain several remarkable features of high-p_T baryon production in heavy ion collisions which have recently been observed at RHIC: (a) the anomalous increase of the proton-to-pion ratio with centrality (b): the increased power-law fall-off at fixed $x_T = 2p_T/\sqrt{s}$ of the charged particle production cross section in high centrality nuclear collisions, and (c): the anomalous decrease of the number of same-side hadrons produced in association with a proton trigger as the centrality increases. These phenomena emphasize the importance of understanding hadronization at the amplitude level in QCD. They also illustrate how heavy ion collisions can provide sensitive tools for interpreting and testing fundamental properties of QCD.

Clearly careful analyses and measurements at RHIC over a wide range of energies is needed to validate or disprove the importance of higher-twist direct reactions in hard ion collisions. The scaling behavior of cross sections and particle ratios at fixed x_T is the most direct measure of multiparton subprocesses. We have also emphasized that strangeness correlations between opposite-side hyperons and kaons can provide a clear signature of higher-twist contributions. Measurements of the associated particles in direct photon production will also be very valuable for understanding these remarkable features of QCD in the nuclear medium.

Acknowledgments:

We thank David Morrison, Michael Tannenbaum, and Werner Vogelsang for helpful comments. This work supported in part by the Department of Energy under contracts DE-AC02-76SF00515 (S.J.B) and DE-AC02-98CH1-886 (A.S.). SLAC-PUB-13224.

References

[1] A. Adare, et al., Phys. Rev. D76 (2007) 051106.

[2] I. Arsene, et al., Nucl. Phys. A757 (2005) 1–27.

[3] B. B. Back, et al., Nucl. Phys. A757 (2005) 28–101.

[4] J. Adams, et al., Nucl. Phys. A757 (2005) 102–183.

[5] K. Adcox, et al., Nucl. Phys. A757 (2005) 184–283.

[6] S. S. Adler, et al., Phys. Rev. Lett. 91 (2003) 172301.

[7] B. I. Abelev, et al., Phys. Lett. B655 (2007) 104–113.

[8] S. S. Adler, et al., Phys. Rev. C71 (2005) 051902.

[9] A. Adare, et al., Phys. Lett. B649 (2007) 359–369.

[10] R. C. Hwa, C. B. Yang, Phys. Rev. C67 (2003) 034902.

[11] V. Greco, C. M. Ko, P. Levai, Phys. Rev. Lett. 90 (2003) 202302.

[12] R. J. Fries, B. Muller, C. Nonaka, S. A. Bass, Phys. Rev. C68 (2003) 044902.

[13] R. J. Fries, S. A. Bass, B. Muller, Phys. Rev. Lett. 94 (2005) 122301.

[14] R. J. Fries, J. Phys. Conf. Ser. 27 (2005) 70–79.

[15] S. J. Brodsky, M. Diehl, P. Hoyer, S. Peigne, Phys. Lett. B449 (1999) 306–312.

[16] E. L. Berger, S. J. Brodsky, Phys. Rev. Lett. 42 (1979) 940–944.

[17] G. P. Lepage, S. J. Brodsky, Phys. Rev. D22 (1980) 2157.

[18] S. J. Brodsky, G. F. de Teramond.

[19] S. M. Berman, J. D. Bjorken, J. B. Kogut, Phys. Rev. D4 (1971) 3388.

[20] S. J. Brodsky, H. J. Pirner, J. Raufeisen, Phys. Lett. B637 (2006) 58–63.

[21] J. Cronin, Proceedings of the SLAC Summer Institute on Particle Physics.

[22] S. S. Adler, et al., Phys. Rev. C69 (2004) 034910.

[23] M. J. Tannenbaum, PoS CFRNC2006 (2006) 001.

[24] S. S. Adler, et al., Phys. Rev. Lett. 98 (2007) 012002.

[25] S. J. Brodsky, G. P. Lepage, P. B. Mackenzie, Phys. Rev. D28 (1983) 228.

[26] M. Binger, S. J. Brodsky, Phys. Rev. D74 (2006) 054016.

[27] R. Blankenbecler, S. J. Brodsky, J. F. Gunion, Phys. Rev. D12 (1975) 3469–3487.

[28] S. J. Brodsky, M. Burkardt, I. Schmidt, Nucl. Phys. B441 (1995) 197–214.

[29] A. V. Efremov, A. V. Radyushkin, Phys. Lett. B94 (1980) 245–250.

[30] D. de Florian, W. Vogelsang, F. Wagner, Phys. Rev. D76 (2007) 094021.

[31] G. Bertsch, S. J. Brodsky, A. S. Goldhaber, J. F. Gunion, Phys. Rev. Lett. 47 (1981) 297.

[32] S. J. Brodsky, A. H. Mueller, Phys. Lett. B206 (1988) 685.

[33] L. Frankfurt, G. A. Miller, M. Strikman, Comments Nucl. Part. Phys. 21 (1992) 1–40.

[34] E. M. Aitala, et al., Phys. Rev. Lett. 86 (2001) 4773–4777.

[35] B. Clasie, et al., Phys. Rev. Lett. 99 (2007) 242502.

[36] B. Mohanty, et al., Quark Matter 2008.

[37] L. Ruan, J. Phys. G34 (2007) S199–206.

[38] S. Albino, B. A. Kniehl, G. Kramer, Nucl. Phys. B725 (2005) 181–206.

[39] X.-N. Wang, Phys. Rev. C58 (1998) 2321.